

# Preparation and photocatalytic application of Zn-Fe<sub>2</sub>O<sub>4</sub>@ZnO core-shell structured spheres

Rahmatollah Rahimi, Mahdi Heidari-Golafzani, Mahboubeh Rabbani\*

*Department of Chemistry, Iran University of Science and Technology, Tehran 16846-13114, Iran,*

*E-mail: M\_rabani@iust.ac.ir*

## Abstract

In this work, nanohollow Zn-Fe<sub>2</sub>O<sub>4</sub> spheres were prepared from ZnCl<sub>2</sub>, FeCl<sub>3</sub>.6H<sub>2</sub>O and ammonium acetate using the hydrothermal method. Then, Zn-Fe<sub>2</sub>O<sub>4</sub>@ZnO core-shell structured spheres were synthesized by using immobilization of ZnO nanoparticles on surface of Zn-ferrite spheres via sol-gel rout. SEM images showed that the Zn-Fe<sub>2</sub>O<sub>4</sub> and Zn-Fe<sub>2</sub>O<sub>4</sub>@ZnO core-shell structured spheres are made of the spherical shape particles. Results of VSM reveal that the Zn-Fe<sub>2</sub>O<sub>4</sub> nanoparticles are superparamagnetic. Photocatalytic activity studies confirmed that as-prepared Zn-Fe<sub>2</sub>O<sub>4</sub>@ZnO core-shell structured spheres had excellent photodegrading behavior to methylene blue (MB) compared to pure ZnO nanoparticles. Also Zn-Fe<sub>2</sub>O<sub>4</sub>@ZnO core-shell structured spheres due to the magnetic properties of environment can be easily removed. Furthermore, Zn-Fe<sub>2</sub>O<sub>4</sub>@ZnO core-shell structured spheres could be also served as convenient recyclable photocatalysts because of their magnetic properties.

**Keywords:** Zn-Fe<sub>2</sub>O<sub>4</sub>@ZnO, Core-shell, Nanohollow spheres, Photocatalyst, MB

## 1. Introduction

Dyes can give various products beautiful colors, and therefore they are widely used in many fields such as textiles, paper, plastic, food, painting, and medicine [1]. Quantities of dye effluent are produced in the dye manufacturing industries and during the dyeing process. According to incomplete statistics, they are more than 10,000 types of dyes in commercial circulation [2]. Dye contamination in wastewater causes problems in several ways: the presence of dyes in water, even in very low quantities, is highly visible and undesirable; color interferes with penetration of sunlight into waters; retards photosynthesis; inhibits the growth of aquatic biota and interferes with gas solubility in water bodies [3,4].

The alarming question is the disposal of effluent discharged by these industries. The basis of ISO- 14000 is mainly for the disposal of residual contents of these industries. But unfortunately the industries are lacking somewhere in following the procedure recommended for this purpose [5].

Some of the worrying problems related to it including. One of the high consuming materials in the dye industry is Methylene Blue (MB) which is used for cotton and silk painting [6]. Chemical structure of MB is illustrated in Fig. 1 [7].

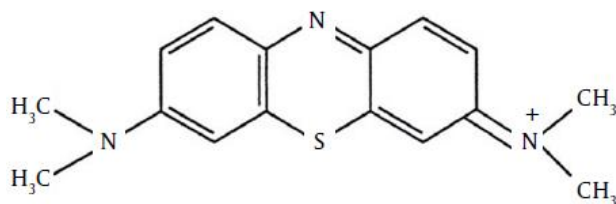


Fig. 1 Schematic structure of methylene blue

The separation and recycling of the photocatalysts are still a serious problem. Fortunately, magnetic separation offers a convenient way to remove and recycle the magnetic composite materials by applying an external magnetic field [8]. Recently, research on core-shell structured nanoparticles has become an active field because of their unique chemical and physical properties and potential applications in many areas [9,10]. ZnO is an important wide band-gap II-IV semiconductor, which has a wide and direct band-gap of 3.37 eV at room temperature with the large exciton binding energy of 60 meV [11].

Although the ZnO nanoparticles have been used as a catalyst for photocatalytic degradation, the Zn-Fe<sub>2</sub>O<sub>4</sub>@ZnO core-shell has not been sufficiently investigated. In the present investigation, a new nanohollow Zn-Fe<sub>2</sub>O<sub>4</sub>@ZnO core-shell catalyst was synthesized to combine both advantages of Zn-Fe<sub>2</sub>O<sub>4</sub> and ZnO.

## 2. Experimental

### 2.1. Materials

In this study, iron (III) chloride (FeCl<sub>3</sub>), zinc chloride (ZnCl<sub>2</sub>), ammonium acetate, ethylene glycol (C<sub>2</sub>H<sub>6</sub>O<sub>2</sub>), zinc acetate (Zn(C<sub>2</sub>H<sub>3</sub>O<sub>2</sub>)<sub>2</sub>·6H<sub>2</sub>O) and ethanol were used to prepare the samples.

## **2.2. Preparation of Zn-Fe<sub>2</sub>O<sub>4</sub> nanoparticles**

A mixture of 70 ml ethylene glycol, iron (III) chloride and zinc chloride was stirred in a mechanic stirrer to achieve a clean solution. Then, the above solution was added during stirring 2.312 g NH<sub>4</sub>Ac. With continued practice of mixing, the color turns to dark yellow and palms appeared. This solution for 40 min was sonicated. The solution is then placed in an oven at 215 °C for 4 h to obtain a black precipitate.

## **2.3. Preparation of Zn-Fe<sub>2</sub>O<sub>4</sub>@ZnO core-shell**

The resulting black precipitation was re-dispersed in deionized water before 0.08 g Zn-Fe<sub>2</sub>O<sub>4</sub> was added to it. Then, we sonicated for 2 h and freeze-thaw action of ammonia added drop wise until the pH reached 11. The precursor solution was transferred into a round-bottom flask and kept at 120 °C for 3 h. After cooled to room temperature, the precipitate was placed in an oven at temperature of 80 °C for 24h and then placed into a vacuum oven at 80 °C for 24 h.

## **2.4. Characterization of Zn-Fe<sub>2</sub>O<sub>4</sub>@ZnO core-shell**

The particle morphologies of the ZnO powder were observed by an AIS2100 (Seron Technology) scanning electron microscopy (SEM). The FT-IR analyses were carried out on a Shimadzu FTIR-8400S spectrophotometer using a KBr pellet for sample preparation. DRS spectra were prepared via a Shimadzu (MPC-2200) spectrophotometer. Also a commercial HH-15 model vibrating sample magnetometer (VSM, Lake Shore 7410) was used at room temperature to characterize the magnetic properties of Zn-Fe<sub>2</sub>O<sub>4</sub> particles and Zn-Fe<sub>2</sub>O<sub>4</sub>@ZnO nanohollow spheres.

## **2.5. Photocatalytic experiments**

Photocatalytic activity studies of the prepared Zn-Fe<sub>2</sub>O<sub>4</sub>@ZnO core-shells were evaluated by the degradation MB solution. LED lamp was used as Shimadzu spectrophotometer devices. Subsequently the mixture was poured into a quartz glass beaker and began the photocatalytic degradation tests. In the experiment, the reaction solution was mixed by magnet stirrer which was placed right under light source.

The concentration of MB was determined by measuring the absorption intensity at its maximum

absorbance wavelength of MB by using a UV-vis spectrophotometer with a 1 cm path length spectrophotometric quartz cell. The degradation percentage of the dyes wastewaters was defined as:

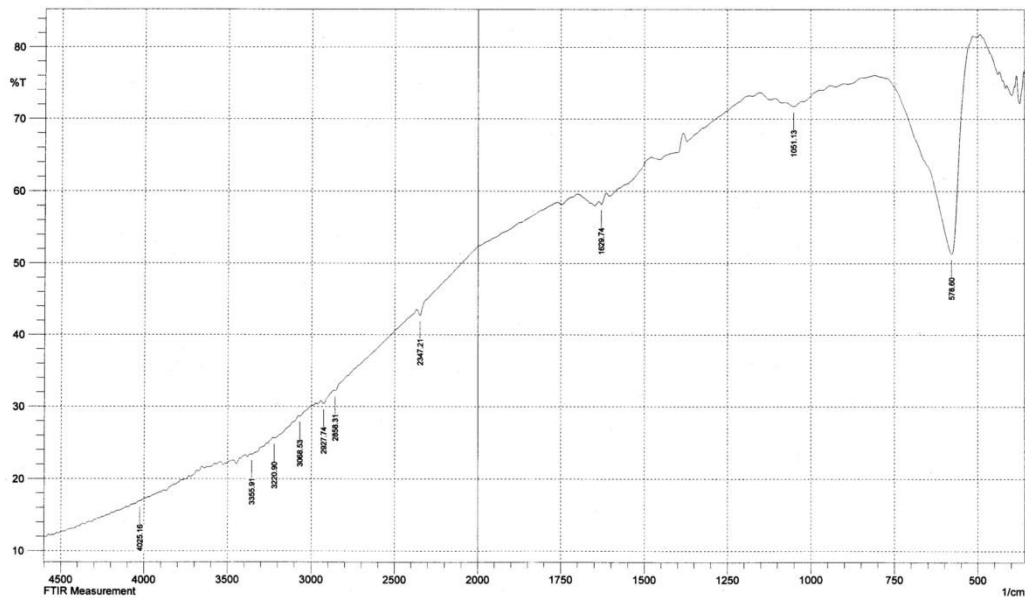
$$PDP = \frac{C_0 - C_t}{C_0} = \frac{A_0 - A_t}{A_0}$$

Where PDP is the abbreviation of the photocatalytic degradation percentage,  $C_0$  is the initial dye concentration;  $C_t$  is the dye concentration at certain reaction time  $t$  (min),  $A_0$  UV-Vis absorption of original solution and  $A_t$  is the UV-vis absorption of degraded solution at the certain minutes [12].

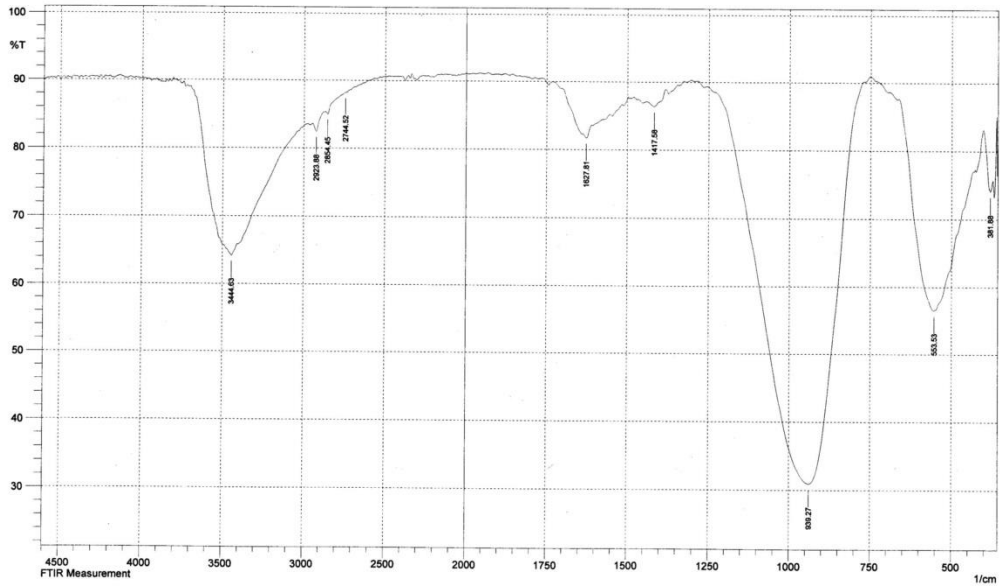
### 3. Results and discussion

#### 3.1. FT-IR spectroscopy

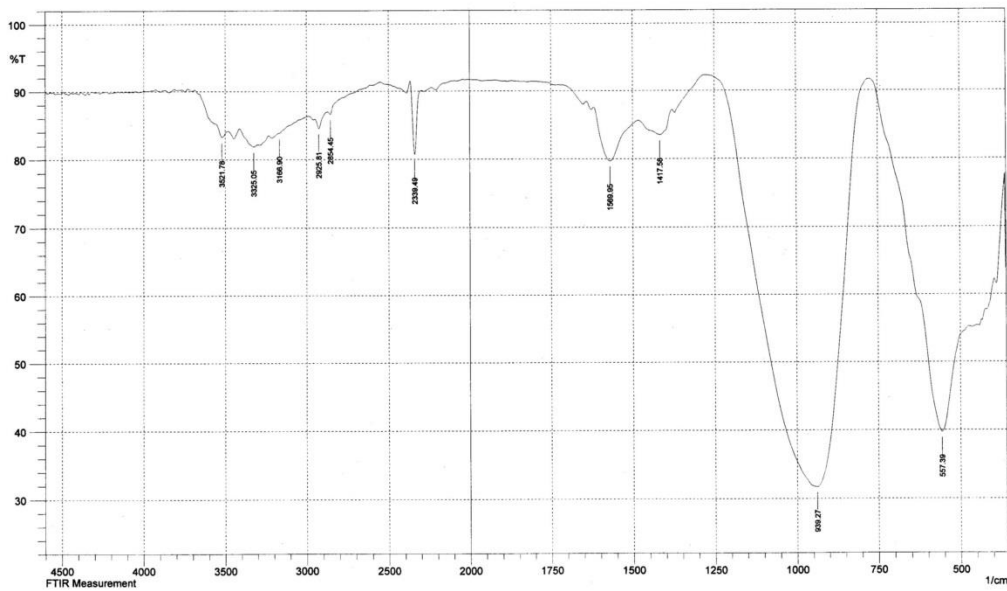
The FT-IR spectra of Zn-Fe<sub>2</sub>O<sub>4</sub>, pure ZnO and composite are shown in Fig. 1.



a



b



c

**Fig. 1.** The FT-IR spectra of a) Zn-Fe<sub>2</sub>O<sub>4</sub>, b) pure ZnO and c) composite

### 3.2. XRD diffraction

Fig. 2 shows the XRD pattern of Zn-Ferrites and ZnO@Zn-Ferrite. The position of all diffraction peaks match well with those of Zn-Fe<sub>2</sub>O<sub>4</sub> peaks at  $2\theta=29.86^\circ$ ,  $35.21^\circ$ ,  $56.68^\circ$ ,  $62.25^\circ$ . The lattice system of Zn-Ferrite is cubic, which is in good agreement with standard card JCPDS No. 22-

1012.

At the XRD patterns of ZnO@Zn-Ferrite, it can be seen that all added peaks are in good agreement with hexagonal (wurtzite) ZnO (JCPDS Card, No. 36-1451).

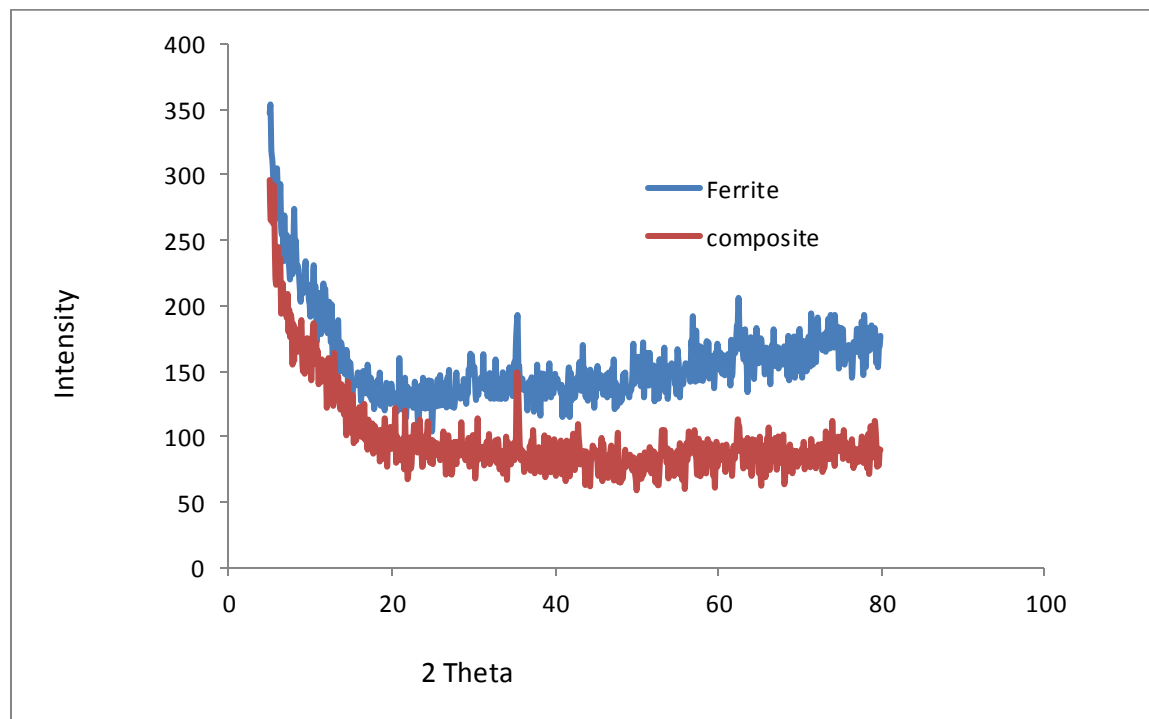


**Fig. 2.** The XRD pattern of Zn-Ferrites and ZnO@Zn-Ferrite

### 3.3. DRS spectroscopy

The optical properties of Zn-Fe<sub>2</sub>O<sub>4</sub> particles and Zn-Fe<sub>2</sub>O<sub>4</sub>@ZnO nanohollow sphere samples were obtained using UV-Vis DRS and their results are shown in Fig. 3. As can be seen Zn-Fe<sub>2</sub>O<sub>4</sub> has absorption in the visible light range, also Zn-Fe<sub>2</sub>O<sub>4</sub>@ZnO nanohollow sphere have strong absorption in this range. Results obtained from two samples are same because Zn-Fe<sub>2</sub>O<sub>4</sub> has much more impact on band-gap than ZnO. For Zn-Fe<sub>2</sub>O<sub>4</sub>@ZnO nanohollow sphere, there is considerable absorption in the visible range confirming that the nanohollow sphere are composed of, Zn-Fe<sub>2</sub>O<sub>4</sub> and ZnO counterparts. Hence, it can be concluded that the nanohollow sphere could have photocatalytic activity under visible light irradiation. The band gap for Zn-Fe<sub>2</sub>O<sub>4</sub> and Zn-Fe<sub>2</sub>O<sub>4</sub>@ZnO particles are shown in Fig. 4.

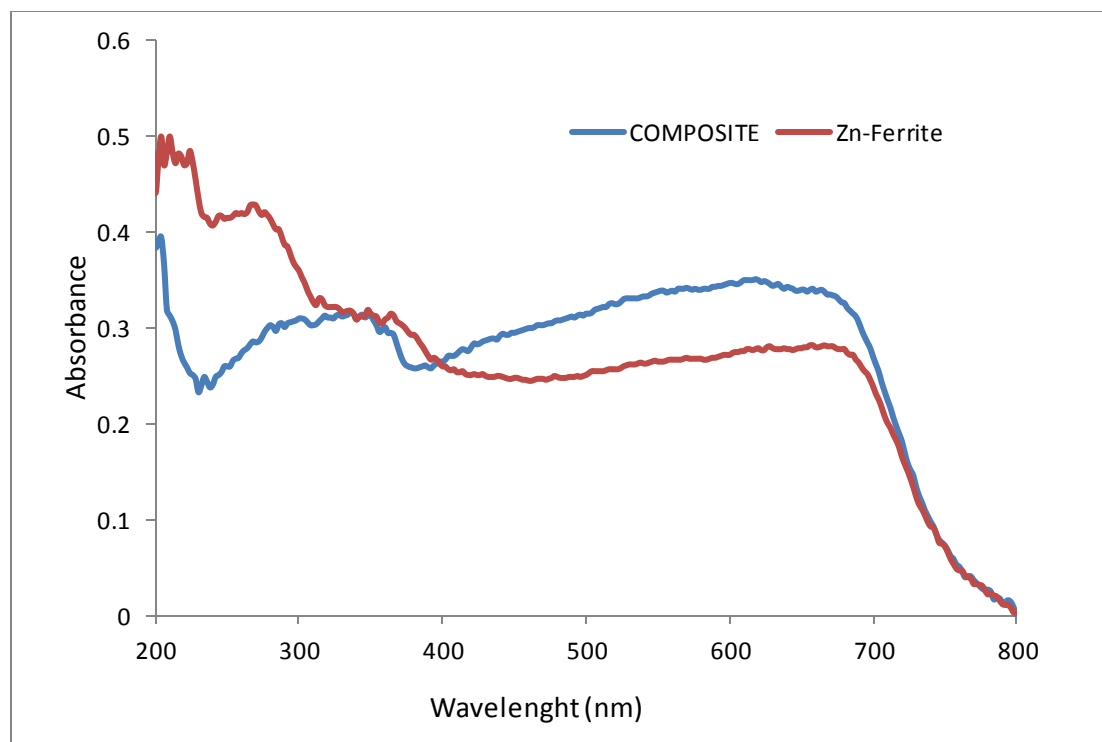


**Fig. 3.** UV-vis DRS for Zn-Fe<sub>2</sub>O<sub>4</sub> and Zn-Fe<sub>2</sub>O<sub>4</sub>@ZnO particles

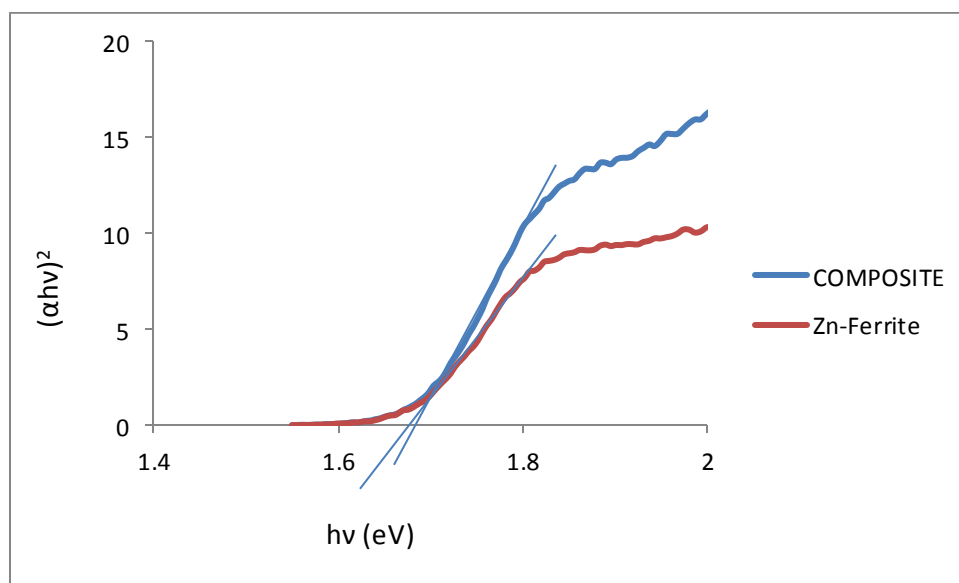


**Fig. 4.** The band gap for Zn-Fe<sub>2</sub>O<sub>4</sub> and Zn-Fe<sub>2</sub>O<sub>4</sub>@ZnO particles

### 3.4. Morphology study

The morphology of the ZnO, Zn-Fe<sub>2</sub>O<sub>4</sub> and Zn-Fe<sub>2</sub>O<sub>4</sub>@ZnO particles from SEM images as shown in Fig. 4. It was found that all Zn-Fe<sub>2</sub>O<sub>4</sub> and Zn-Fe<sub>2</sub>O<sub>4</sub>@ZnO nanohallowsphere were quit

uniform in size. but it happened in case of ZnO sintering of particles and particle size is not uniform. Fig1 a,b,c show image of the Zn-Fe<sub>2</sub>O<sub>4</sub>, Zn-Fe<sub>2</sub>O<sub>4</sub>@ZnO and pure ZnO.

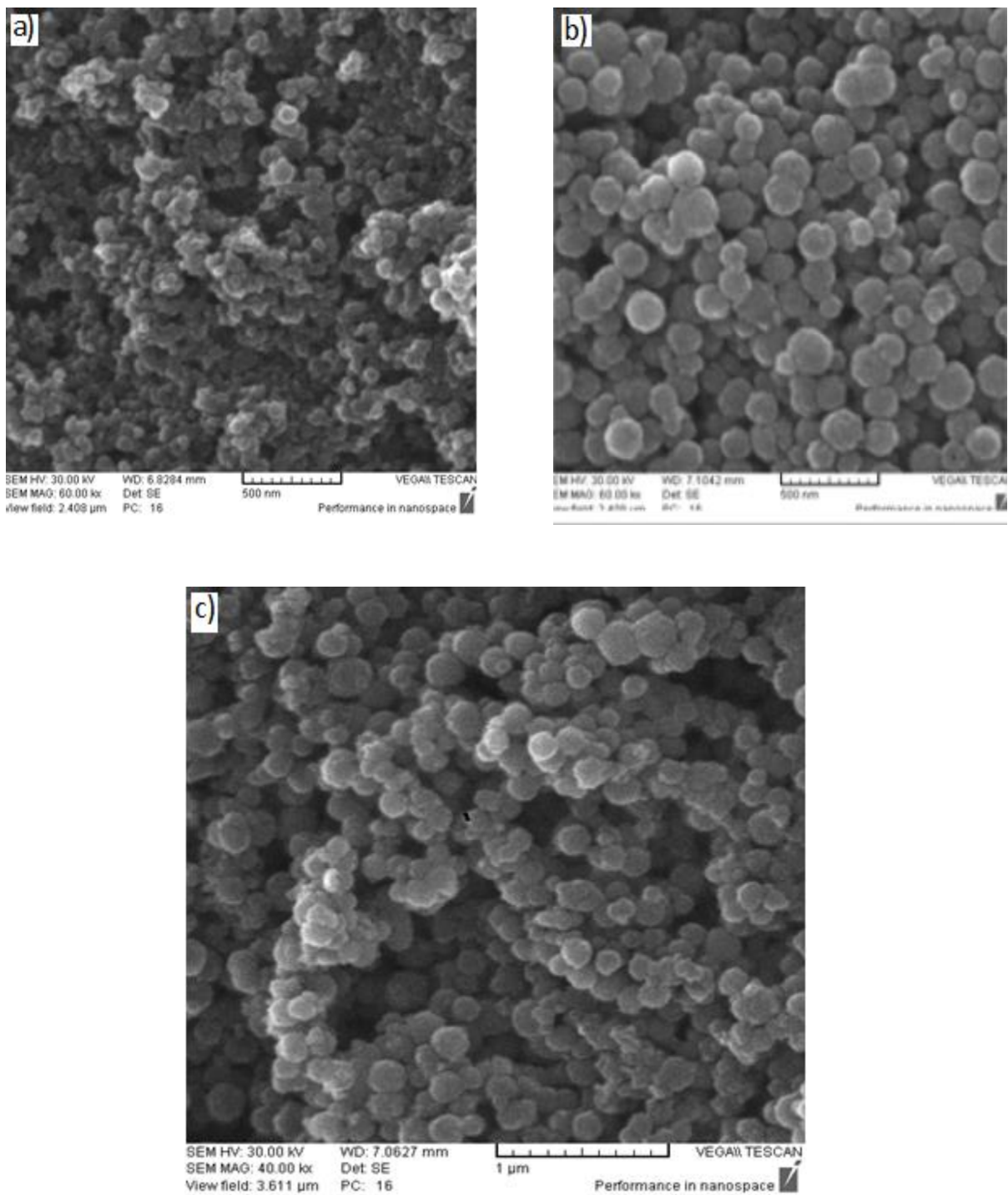


**Fig. 5.** The SEM images of a) ZnO, b) Zn-Fe<sub>2</sub>O<sub>4</sub> and c) Zn-Fe<sub>2</sub>O<sub>4</sub>@ZnO



### 3.5. Magnetic characterization

The magnetic hysteresis loops for the synthesized sample is shown in Fig. 6. The magnetic properties of the hollow ferrites were analyzed by room temperature vibrant sample magnetometer (VSM) with an applied  $-7.3 \leq H \leq 7.3$  KOe field. According to the mentioned curve, the value of saturation magnetization ( $M_s$ ) and the remnant magnetization ( $M_r$ ) are 76.2, 17.79 emu/g respectively. The coercivity field is 95.5 Oe which clearly indicates that the synthesized nanoparticles have weak ferromagnetic behavior, with slender hysteresis curve. It can be inferred from the hysteresis loops that the hollow nanospheres are magnetically soft at room temperature. In addition, the hollow Zn-Fe<sub>2</sub>O<sub>4</sub> synthesized by this method shows the better magnetic properties to other counterparts prepared by template polymerization. It can be attributed to smaller size of spheres either diameter or hollows dimension.

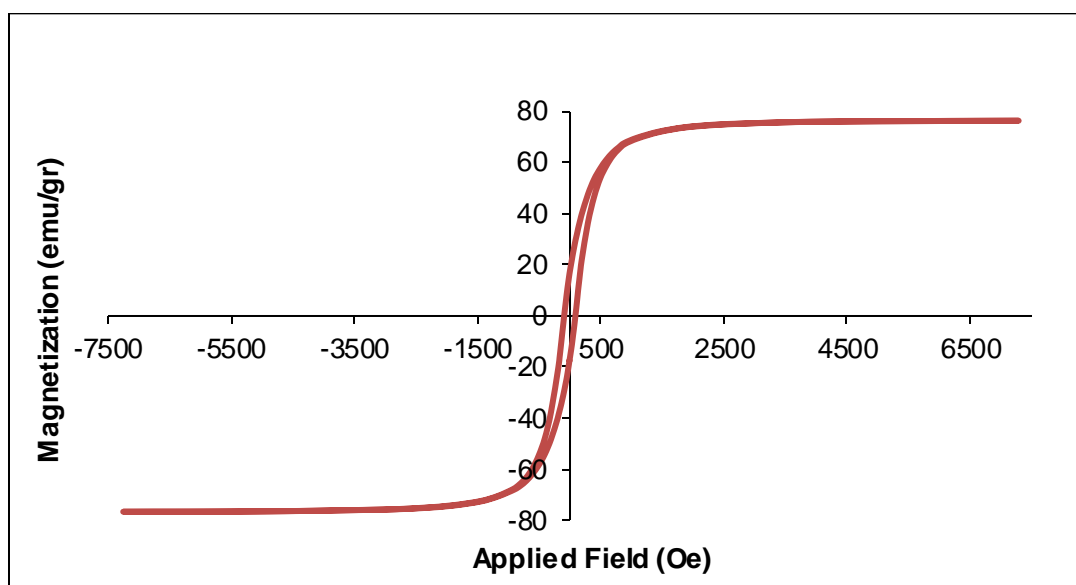
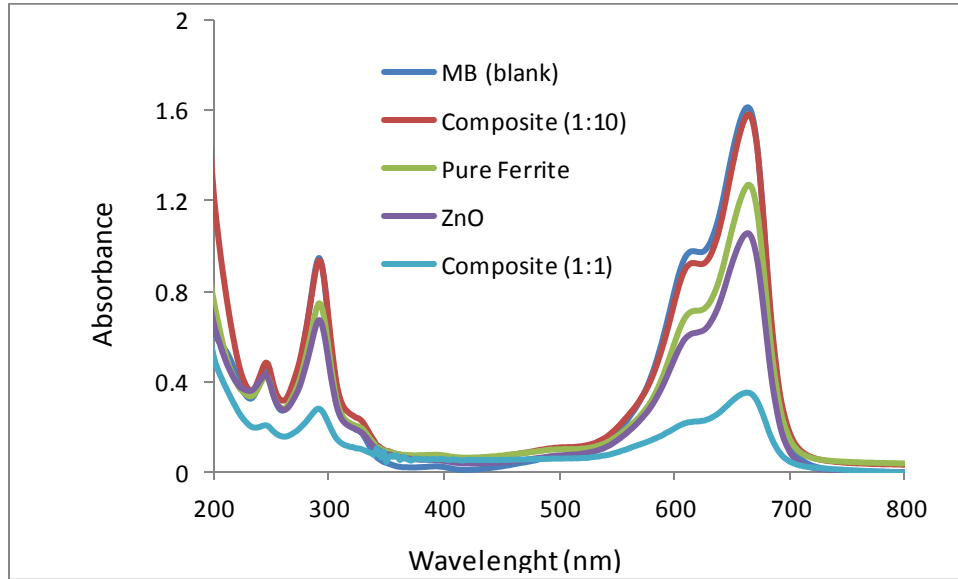


**Fig. 6.** The magnetic hysteresis loops for the synthesized nanohollow Zn-Fe<sub>2</sub>O<sub>4</sub> sphere

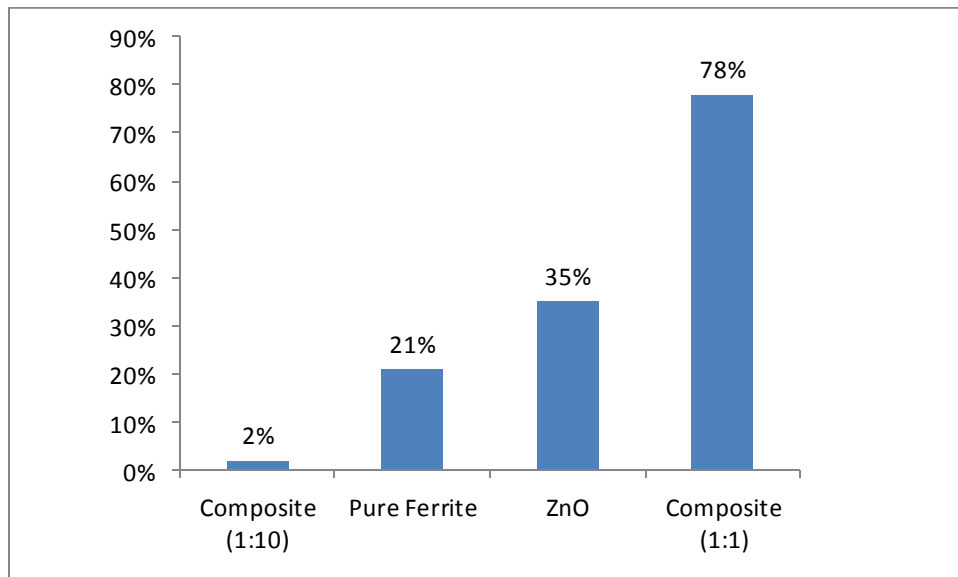
### 3.6. Photocatalytic degradation of methylene blue

Fig. 7 shows effect of molar ratio of nanohollow sphere, the dosage of catalysts and the initial concentration of MB were tested in our work. In order to throw light on the subject, blank experiment was carried out for the dye solution without catalysts and no significant degradation was observed. In similar, the blank experiment in presence of ZnO was observed offer a period of 3 h. The above result indicate the /both light and/ catalyst are essential for the effective

removal of dyes. Removal efficiency of MB photodegradation by ZnO, Zn-Fe<sub>2</sub>O<sub>4</sub>, Zn-Fe<sub>2</sub>O<sub>4</sub>@ZnO (1:1) and Zn-Fe<sub>2</sub>O<sub>4</sub>@ZnO (1:10) is shown in Fig. 8.



**Fig. 7.** UV-vis spectra for degradation of MB under visible light irradiation on ZnO, Zn-Fe<sub>2</sub>O<sub>4</sub>, Zn-Fe<sub>2</sub>O<sub>4</sub>@ZnO (1:1) and Zn-Fe<sub>2</sub>O<sub>4</sub>@ZnO (1:10)



**Fig. 8.** Removal efficiency of MB photodegradation by ZnO, Zn-Fe<sub>2</sub>O<sub>4</sub>, Zn-Fe<sub>2</sub>O<sub>4</sub>@ZnO (1:1) and Zn-Fe<sub>2</sub>O<sub>4</sub>@ZnO (1:10)

#### 4. Conclusions

Magnetically separable Zn-Fe<sub>2</sub>O<sub>4</sub>@ZnO nanohollow sphere as visible-light-driven photocatalysts, were prepared by refluxing mixtures of Zn-Fe<sub>2</sub>O<sub>4</sub> with related inorganic salt of zinc. Visible light photocatalytic activity of the nanohollow sphere was investigated by degradation of MB. In order to investigate the effect of ZnO content on the photocatalytic activity, a series of the nanocomposites with different weight ratios of core-shell and also pure ZnO and Zn-Fe<sub>2</sub>O<sub>4</sub> were prepared. The nanohollow sphere with 1:1 weight ratio has superior activity in degradation of MB. After visible light irradiation for 3 h, about 78% of MB molecules were degraded on Zn-Fe<sub>2</sub>O<sub>4</sub>@ZnO (with molar ratio of 1:1) nanohollow sphere that is much better than the other samples.

#### References:

- [1] Sajab, M. S., Chia, C. H., Zakaria, S., Jani, S. M., Ayob, M. K., Chee, K.L., Khiew, P. S., And Chiu, W. S. (2011). "Citric acid modified kenaf core fibres for removal of methylene blue from aqueous solution," *Bioresource Technology* 102, 7237-7243.
- [2] Altinisik, A., Gur, E., and Seki, Y. (2010). "A natural sorbent, Luffa cylindrical for the removal of a model basic dye," *Journal of Hazardous Materials* 179, 658-664.
- [3] Garg VK, Amita M, Kumar R, Gupta R (2004). Basic dye (methylene blue) removal from simulated wastewater by adsorption using Indian rosewood sawdust: a timber industry waste. *Dyes Pigments* 63:243–250.
- [4] Robinson T, Chandran B, Nigam P (2002). From an artificial textile dye effluent by two agricultural waste residues, corn cob and barley husk. *Environ. Int.* 28: 29-33.
- [5] Khan, AR; Tahir H; Uddin, F; Waqar, S (2004) Adsorption of methylene blue and malachite green on the surface of wool carbonizing waste. *Saudi. J. Chem. Soc.* (Submitted).
- [6] Yang J, Qiu K. Preparation of activated carbons from walnut shells via vacuum chemical activation and their application for methylene blue removal. *Chem Eng J.* 2010; **165**(1):209–17.
- [7] Iqbal MJ, Ashiq MN. Adsorption of dyes from aqueous solution on activated charcoal. *J Hazard Mater.* 2007; **139**(1):57–66.
- [8] W. Chiu, P. Khiew, M. Cloke, D. Isa, H. Lim, T. Tan, et al., *Journal of Physical Chemistry C* 114 (2010) 8212–8218.

- [9] Y. Jun, J. Choi, J. Cheon, Heterostructure magnetic nanoparticles: their versatility and high performance capabilities. *Chem. Commun.* (2007) 1203.
- [10] C. Lin, Y. Li, M. Yu, P. Yang, J. Lin, Adv. A facile synthesis and characterization of monodisperse spherical pigment particles with a core/shell structure. *Funct. Mater.* 17 (2007) 1459.
- [11] T. Fukumura, Z. Jin, A. Ohtomo, H. Koinuma, M. Kawasaki, High throughput fabrication of transition-metal-doped epitaxial ZnO thin films: A series of oxide-diluted magnetic semiconductors and their properties, *Appl. Phys. Lett.* 75 (1999) 3366.
- [12] Juan Xia, Anqi Wang, Xiang Liu, Zhongxing Su. Preparation and characterization of bifunctional, Fe<sub>3</sub>O<sub>4</sub>/ZnO nanocomposites and their use as photocatalysts. *Applied Surface Science* 257 (2011) 9724–9732.